ELSEVIER

PII: S0021-9290(97)00071-7

J. Biomechanics, Vol. 30, No. 10, pp. 1051–1058, 1997

Printed in Great Britain
0021-9290/97 $17.00 + .00

THE EFFECT OF PEDALING RATE ON COORDINATION IN CYCLING

R. R. Neptune,* S. A. Kautz† and M. L. Hull*‡

* Department of Mechanical Engineering, University of California, Davis, CA 95616, U.S.A; and † Rehabilitation R&D Center (153), Department of Veterans Affairs, Palo Alto Health Care System, Palo Alto, CA 94304, U.S.A.

Abstract—To further understand lower extremity neuromuscular coordination in cycling, the objectives of this study were to examine the effect of pedaling rate on coordination strategies and interpret any apparent changes. These objectives were achieved by collecting electromyography (EMG) data of eight lower extremity muscles and crank angle data from ten subjects at 250 W across pedaling rates ranging from 45 to 120 RPM. To examine the effect of pedaling rate on coordination, EMG burst onset and offset and integrated EMG (iEMG) were computed. In addition, a phase-controlled functional group (PCFG) analysis was performed to interpret observed changes in the EMG patterns in the context of muscle function. Results showed that the EMG onset and offset systematically advanced as pedaling rate increased except for the soleus which shifted later in the crank cycle. The iEMG results revealed that muscles responded differently to increased pedaling rate. The gastrocnemius, hamstring muscles and vastus medialis systematically increased muscle activity as pedaling rate increased. The gluteus maximus and soleus had significant quadratic trends with minimum values at 90 RPM, while the tibialis anterior and rectus femoris showed no significant association with pedaling rate. The PCFG analysis showed that the primary function of each lower extremity muscle remained the same at all pedaling rates. The PCFG analysis, which accounts for muscle activation dynamics, revealed that the earlier onset of muscle excitation produced muscle activity in the same region of the crank cycle. Also, while most of the muscles were excited for a single functional phase, the soleus and rectus femoris were excited during two functional phases. The soleus was classified as an extensor-bottom transition muscle, while the rectus femoris was classified as a top transition-extensor muscle. Further, the relative emphasis of each function appeared to shift as pedaling rate was increased, although each muscle remained bifunctional. © 1997 Elsevier Science Ltd

Keywords: Muscle coordination; Electromyography; Cycling; Pedaling rate.

INTRODUCTION

Coordination of the lower extremity muscles during cycling has been investigated experimentally (e.g. Ryan and Gregor, 1992) and theoretically in forward dynamic simulation studies (e.g. Raasch *et al.*, 1997). Pedaling is an ideal task for studying muscle coordination since it is a constrained cyclical movement which allows controlled investigation of test conditions such as movement speed. Movement speed can be systematically controlled by pedaling rate to examine how the central nervous system responds to changing workloads and dynamic interactions within the musculoskeletal system.

Previous research suggests that the timing of muscular excitation as pedaling rate changes may reveal principles underlying muscular coordination. As pedaling rate increases, significant linear trends for peak EMG to shift earlier in the crank cycle have been reported in various muscles (Marsh and Martin, 1995). Based on this finding, these authors hypothesized that muscle excitation must occur progressively earlier in the crank cycle as pedaling rate increases in order to develop pedal force in the same region. Since previous studies on the EMG-pedaling rate relationship have neither quantified changes in burst onset and offset (Ericson *et al.*, 1985; Marsh and Martin, 1995), nor done so over an extensive range of pedaling rates (Suzuki *et al.*, 1982), this hypothesis has not been tested.

In addition to muscular excitation timing, the magnitude (integrated EMG — iEMG) may also be important in the study of pedaling coordination. Investigators have quantified both peak EMG activity (Ericson *et al.*, 1985; Marsh and Martin, 1995) and iEMG-based measures (Citterio and Agostini, 1984; Goto *et al.*, 1976; Marsh and Martin, 1995; Takaishi *et al.*, 1994) in various muscles across different pedaling rates. Results have indicated different trends in excitation for muscles within the same group (e.g. triceps surae) suggesting that these muscles may be coordinated differently as pedaling rate increases.

To explain both muscle function and interpret observed changes in either EMG timing or magnitude, a theoretical framework is necessary. Recent theoretical analyses involving forward simulations (e.g. Raasch *et al.*, 1997) have shown that muscles function primarily through either the downstroke, the upstroke or one of the two transition regions (top- and bottom-dead-center in the crank cycle). Cycling has been simulated by partitioning muscles into four corresponding phase-controlled functional groups (PCFG) (Raasch *et al.*, 1997). Using an analysis based on the four functional phases (the percent of the total iEMG that occurred in each phase), Brown *et al.* (1995) identified pathological muscle function during pedaling by post-stroke subjects with unilateral lower extremity dysfunction. Thus, this analysis would be useful as a theoretical framework for interpreting the importance of observed changes in either EMG timing or magnitude in the context of muscle function.

Received in final form 12 *November* 1996.

‡ Address correspondence to: Professor M. L. Hull, Chair of Biomedical Engineering, Department of Mechanical Engineering, University of California, Davis, CA 95616, U.S.A.

The objectives of this study were threefold. The first objective was to examine the effect of pedaling rate on coordination by testing the hypothesis that EMG patterns defined by burst onset and offset timing and iEMG were affected by changes in pedaling rate. If changes were detected, then the second objective was to test the hypothesis that activation dynamics were the primary cause of these changes. Accepting this hypothesis would suggest that shifts in muscle activity were primarily the result of a phase advance to account for the activation dynamics rather than indicative of a change in muscle function. The final objective was to use the PCFG analysis to interpret both timing and magnitude changes in the context of muscle function.

METHODS

Ten male competitive cyclists volunteered for participation in this study (height = 1.81 ± 0.04 m; mass = 76.49 ± 3.35 kg; age = 29.6 ± 4.1 yr). Informed consent was obtained before the experiment. The subjects rode a conventional racing bicycle with clipless pedals adjusted to match their own bicycle's geometry. The bicycle was mounted on an electronically braked Schwinn Velodyne ergometer which provided a constant workrate independent of pedaling rate. The protocol consisted of a 15 min warm-up period at a workrate of 120 W at 90 RPM. Then, each subject cycled at a workrate of 250 W at six different pedaling rates (45, 60, 75, 90, 105 and 120 RPM) randomly assigned to control for possible interactions and fatigue. After a 3 min adaptation period, data collection was randomly initiated twice during the following 2 min for 10 s each.

The angular orientation of the crank arm was measured with an optical encoder and sampled at 100 Hz. The encoder data were filtered using a fourth-order zero-phase-shift Butterworth low-pass filter with a cut-off frequency of 6 Hz.

Electromyographic (EMG) data of the soleus (SOL), medial gastrocnemius (GAS), tibialis anterior (TA), vastus medialis (VAS), rectus femoris (RF), medial hamstring (SM), biceps femoris (BF), and gluteus maximus (GMAX) were collected on the right leg using pairs of surface electrodes (3 cm center-to-center). Electrode placements were determined based on the work of Delagi *et al.* (1975). The skin was shaved, abraded, and cleaned with isopropyl alcohol to reduce the source impedance. The EMG signals were preamplified with a gain of 850, high-pass filtered with a cut-off frequency of 12 Hz and sampled at 1000 Hz. The raw EMG data were demeaned, full-wave rectified and normalized to the highest value achieved during a series of 10 maximum voluntary isometric contraction (MVC) tests on and off the bicycle (Neptune, 1996). Each test was performed 3 times to elicit the maximum EMG signal. The MVC for each muscle was determined from the maximum signal achieved across all tests. Then, the EMG data were filtered using a root-mean-square (RMS) algorithm with a 40 ms moving rectangular window.

EMG data were further processed to compute burst onset and offset. First, the resting baseline for each muscle was determined after all testing was completed. With the subject in a supine position, data were collected for 10 s and averaged. The burst onset and offset angles were identified using Datapac II (RUN Technologies, Laguna Hills, CA), an automated waveform processing program. The criteria for the onset and offset values were based on a minimum threshold of 3 standard deviations of the resting baseline and a minimum burst duration of 50 ms. Results were then examined interactively on a cycle-by-cycle basis and the threshold was increased when necessary to identify the burst onset and offset. The integrated EMG (iEMG) quantity was computed between the identified burst onset and offset. The cycles were then averaged and divided by the time per cycle yielding units of %MVC. This differs slightly from average EMG, in that activity outside the burst was not included.

The PCFG analysis commenced by computing the integrated muscle activation (iACT) to account for the activation dynamics inherent in muscle stimulation. The activation dynamics were represented by a first-order model with activation and deactivation time constants of 20 and 65 ms, respectively (e.g. Raasch *et al.*, 1997; Winters and Stark, 1988). The functional regions were defined by the work of Raasch *et al.* (1997) relative to top-dead-center (TDC). The Extensor (E) and Flexor (F) regions were defined from 337° to 134° and 149° to 324°, respectively (Fig. 1). The Top (T) and Bottom (B) regions were defined from 241° to 35° and 72° to 228°, respectively. Similar to Brown *et al.* (1995), additional regions were defined in this study as the union between adjacent regions as B–F, E–B, F–T, and T–E to identify bifunctional muscles. Percentages of the whole-cycle iACT within each of the eight regions were computed. Primary muscle function was first identified within the E, F, T, and B groups by the region with the greatest percentage of iACT. Next, the muscle function was redefined as bifunctional if the iACT in any of the additional regions (B–F, E–B, F–T or T–E) exceeded the maximum of the

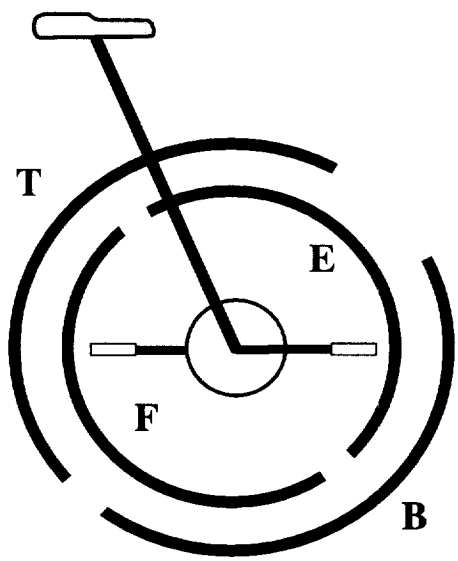

Fig. 1. The phase-controlled functional regions were defined relative to top-dead-center (TDC) based on the work of Raasch *et al.* (1997). The regions were defined as Extensor (E), Flexor (F), Top (T) and Bottom (B). The right crank arm is shown at 90° relative to TDC.

E, F, T and B regions by 20%. All quantities were computed on a cycle-by-cycle basis and averaged across cycles for each subject.

A variety of statistical procedures was used to assess the effects of pedaling rate on the dependent variables of interest. To examine if there were any pedaling rate effects on EMG onset, offset and iEMG data, the statistical analysis consisted of an analysis of variance, using a repeated measures design. This analysis was performed separately for each muscle and dependent variable yielding a total of 24 analyses (8 muscles, 3 variables each). When significant effects were detected ($p < 0.05$), a *post-hoc* Tukey pairwise comparison was used to identify which pedaling rates were significantly different ($p < 0.05$). An orthogonal polynomial decomposition (SAS/STAT User's Guide) was performed to identify either significant linear or quadratic trends in the onset, offset and iEMG data ($p < 0.05$) as a function of pedaling rate. To test the hypothesis that changes in muscle onset are primarily the result of activation dynamics, a second analysis of variance using a repeated measures design was performed to assess the muscle effect on the difference between the burst onset at 45 and 120 RPM. When significant effects were detected, a *post-hoc* Tukey pairwise comparison was used to identify which muscles were significantly different from the others ($p < 0.05$).

RESULTS

The hypothesis that EMG burst onset and offset timing was affected by changes in pedaling rate was supported. The effects of pedaling rate on EMG burst timing were apparent from both graphical and statistical results. The average EMG patterns [Figs 2(a)–(h)] indicate that the burst pattern of each muscle was generally consistent across pedaling rates with some changes in magnitude and timing. The statistical analysis found a significant pedaling rate effect for all muscles on the burst onset except TA ($p = 0.34$), and offset except RF ($p = 0.09$) and TA ($p = 0.59$).

The *post-hoc* orthogonal polynomial decomposition identified a significant linear trend in the burst onset for all muscles except TA and GAS (Table 1). All significant trends shifted the burst onset earlier in the crank cycle except SOL which exhibited a small but significant linear trend towards a later shift. GAS had a significant quadratic trend with the latest onset occurring at the 60 RPM pedaling rate. As pedaling rate was increased past 60 RPM, GAS onset systematically shifted earlier in the crank cycle similar to the other muscles.

The burst offset analysis revealed significant linear trends in all muscles except RF and TA (Table 2). Again, all trends systematically shifted the offset earlier in the crank cycle. GMAX also had a significant quadratic

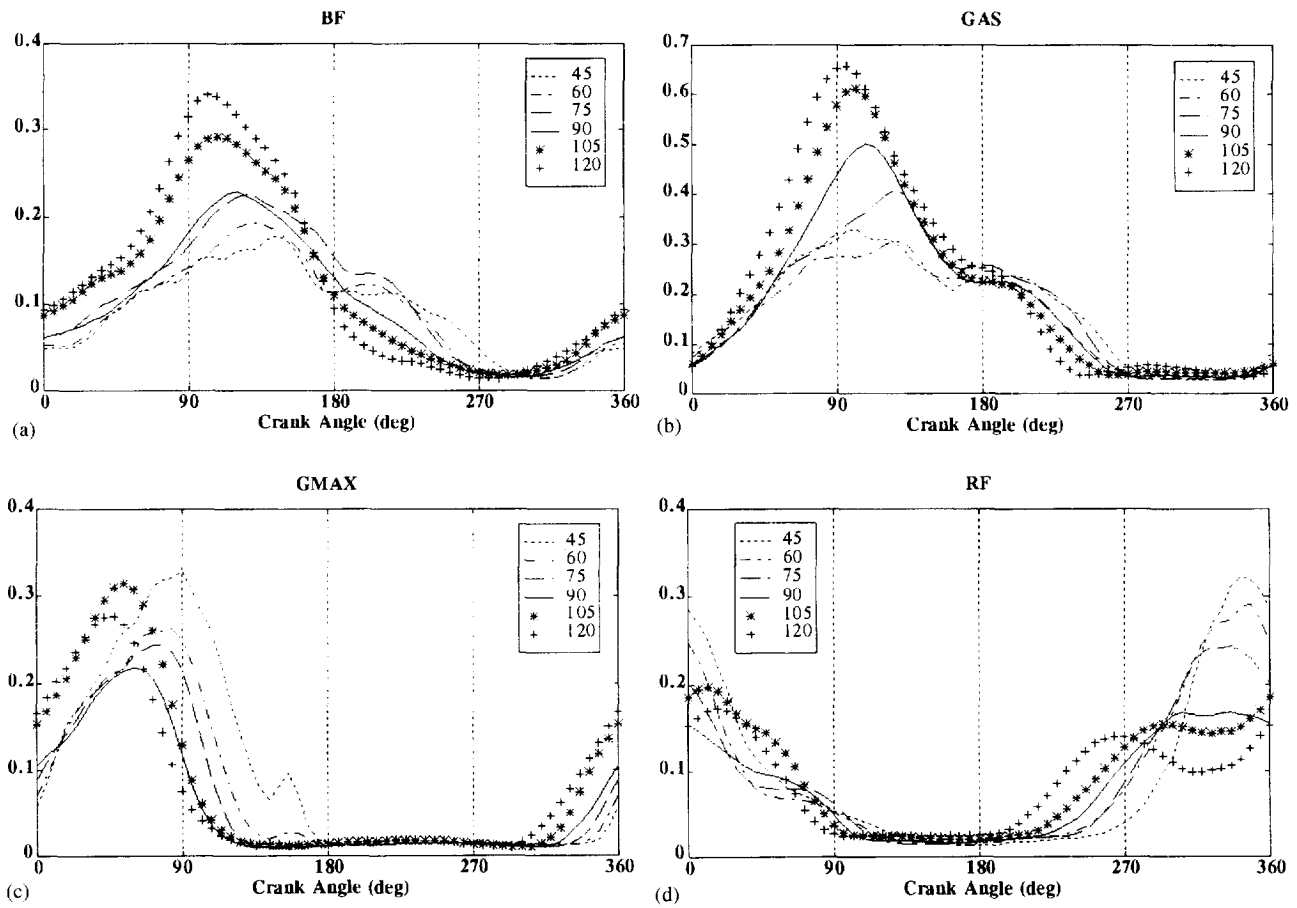

Fig. 2. Normalized electromyographic (EMG) patterns of eight lower extremity muscles across pedaling rates at 45–120 RPM at a constant power output of 250 W. Each curve is the average of ten subjects expressed as a function of crank angle (0–360°).

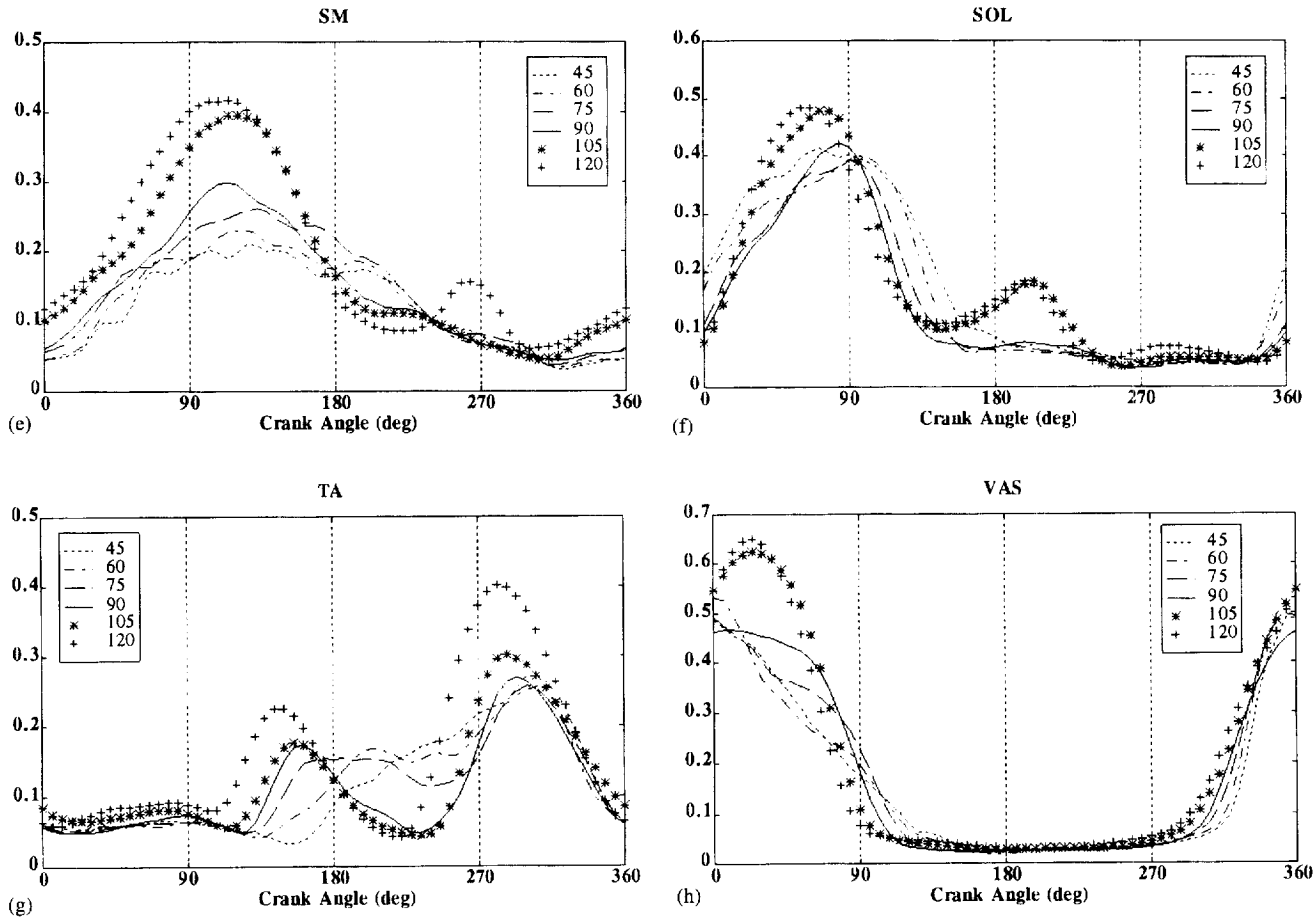

Fig. 2. (Continued)

Table 1. The average crank angle (±1 S.D.) of muscle burst onset for the six different pedaling rates

	Pedaling rate (RPM)					
Muscle	45	60	75	90	105	120
BF*	54 ± 48	42 ± 40	28 ± 41	18 ± 46	15 ± 36	359 ± 31
GAS†‡	18 ± 24	24 ± 22	21 ± 21	19 ± 26	11 ± 20	4 ± 16
GMAX*	358 ± 8	350 ± 10	343 ± 10	331 ± 12	320 ± 12	306 ± 13
RF*	291 ± 15	276 ± 23	270 ± 20	251 ± 24	246 ± 26	226 ± 35
SM*	54 ± 44	44 ± 42	38 ± 43	28 ± 29	11 ± 31	3 ± 36
SOL*‡	346 ± 9	346 ± 10	352 ± 10	349 ± 20	357 ± 10	356 ± 10
TA	185 ± 42	177 ± 40	168 ± 55	193 ± 71	166 ± 69	160 ± 61
VAS*	313 ± 20	312 ± 14	304 ± 15	294 ± 18	293 ± 19	283 ± 22

* Significant linear trend ($p < 0.05$).
† Significant quadratic trend ($p < 0.05$).
‡ Significantly different shift from other muscles in onset between 45 and 120 RPM ($p < 0.05$).
Note: Units are in degrees. Crank angle is defined as 0° at top-dead-center and positive in the clockwise direction. A significant linear or quadratic trend only indicates that the trend (slope) of the data is significantly different from zero. Thus, the statistical analysis may reveal both a linear and quadratic trend for a single data set.

trend as a result of substantial differences in the burst offset between 45 and 60 RPM but still systematically shifted earlier in the crank cycle as pedaling rate increased. SOL also had a quadratic trend with the minimum at 90 RPM.

Visual inspection of the data (Fig. 2) and statistical analysis of the iEMG (Table 3) revealed that the muscles responded differently to increased pedaling rate. The GAS, BF, and SM increased their excitation dramatically when pedaling rate increased (Fig. 2), and these three muscles were found to have a significant linear association, as did VAS (Table 3). GMAX and SOL were found to have quadratic associations with pedaling rate, with the minimum occurring at 90 RPM for each muscle

Table 2. The average crank angle (± 1 S.D.) of muscle burst offset for the six different pedaling rates

Muscle	Pedaling rate (RPM)					
	45	60	75	90	105	120
BF*	222 ± 41	223 ± 26	225 ± 25	199 ± 29	183 ± 20	173 ± 14
GAS*	235 ± 25	227 ± 18	237 ± 16	216 ± 31	211 ± 26	206 ± 14
GMAX*†	148 ± 16	124 ± 16	110 ± 6	102 ± 7	102 ± 12	95 ± 14
RF	50 ± 26	58 ± 42	56 ± 37	77 ± 25	69 ± 16	65 ± 9
SM*	211 ± 62	205 ± 46	205 ± 50	177 ± 42	169 ± 39	172 ± 33
SOL†	166 ± 35	143 ± 9	135 ± 11	132 ± 24	171 ± 59	162 ± 57
TA	335 ± 37	327 ± 35	322 ± 42	332 ± 32	328 ± 44	319 ± 46
VAS*	102 ± 26	99 ± 26	101 ± 9	94 ± 8	83 ± 10	74 ± 6

* Significant linear trend ($p < 0.05$).
† Significant quadratic trend ($p < 0.05$).
Note: Units are in degrees. All muscles had significant linear trends that shifted the burst offset earlier in the crank cycle except the RF and TA.

Table 3. The average muscle integrated electromyogram (iEMG) for the six different pedaling rates

Muscle	Pedaling rate (RPM)					
	45	60	75	90	105	120
BF*	5.7	6.2	7.6	6.8	8.5	10.1
GAS*	11.5	10.4	12.6	13.0	14.7	16.2
GMAX†	7.0	5.4	4.9	4.2	6.0	5.6
RF	6.1	6.2	5.7	5.5	6.1	5.6
SM*	6.8	7.3	8.4	7.8	10.0	10.4
SOL†	12.0	10.3	8.9	8.5	11.0	10.6
TA	7.0	7.0	7.3	6.2	7.3	9.6
VAS*	10.8	11.1	12.0	12.3	14.0	13.8

* Significant linear trend ($p < 0.05$).
† Significant quadratic trend ($p < 0.05$).
Note: Units are in %MVC. BF, GAS, SM and VAS had significant linear trends which generally increased as pedaling rate increased. GMAX and SOL had significant quadratic trends with minimum values occurring at the 90 RPM pedaling rate.

(Table 3). In SOL, the changes in iEMG were consistent with a secondary burst between 135° and 235° that characterized the two highest pedaling rates (Fig. 2). TA and RF had no significant association with pedaling rate. The TA EMG pattern had the greatest variability both within and across subjects, with some subjects exhibiting a two-burst pattern, while others exhibited a single burst pattern.

Muscle function characterized by the PCFG analysis was consistent with the qualitative inspection of the EMG profiles (Fig. 2). At 45 RPM, the analysis defined all muscles with single functions except RF and SOL which were defined as T–E and E–B, respectively. Both RF and SOL had over 90% of all burst activity occurring during these respective regions [Figs 3(d) and (f)]. GMAX and VAS were excited primarily during the extensor region (330°–130°) characterizing them as E muscles [Figs 3(c) and (h)]. The hamstrings (HAMS), BF and SM, and GAS were active primarily from 90° to 270° thus characterizing them as B muscles [Figs 3(a), (e) and (b)]. The only muscle characterized as a T muscle was TA with its primary burst of activity occurring between 225° and 360° [Fig. 2(g)]. Based on this analysis, no muscles were classified as F, B–F or F–T. As pedaling rate was increased to 120 RPM, the primary function of each muscle remained unchanged [Fig. 3].

DISCUSSION

The general objective of this research was to further understand neuromuscular coordination in cycling by investigating the effect of pedaling rate on coordination and interpreting any detected changes. To achieve this objective, EMG of eight lower extremity muscles and bicycle kinematics were collected from ten subjects across six different pedaling rates. To identify changes in coordination, both the burst onset/offset and the iEMG analyses were performed using the EMG data. A PCFG analysis was also performed to aid in the interpretation of any observed changes in the EMG patterns and to identify possible changes in muscle function. Procedural aspects of each of these analyses merit discussion because of the possible influence on results.

Fundamental to the accuracy of identifying the burst onset/offset were the criteria used in the automated waveform processing program. Several combinations of criteria used in previous research (e.g. Bogey *et al.*, 1992; DiFabio, 1987) based on standard deviations of resting baseline, percentages of MVC, and minimum burst duration were evaluated to identify the temporal characteristics of muscle activity. No systematic method reliably identified the on/off burst timing because of the variability of the EMG signal across muscles and subjects. The approach taken in this study was to use the automated waveform processing program with an interactive visual inspection. The on/off burst threshold was systematically increased to identify the primary temporal burst characteristics when the burst off duration did not fall within 3 standard deviations of the resting baseline. This analysis was repeated with a different analyst and the results were found to be insensitive to the analyst using this methodology.

The sensitivity of PCFG analysis results to the activation and deactivation time constants was also examined. The PCFG analysis was designed to minimize the uncertainties inherent in the relationship between muscle excitation and activation by including gaps between immediately adjacent regions (Fig. 1). This results in the

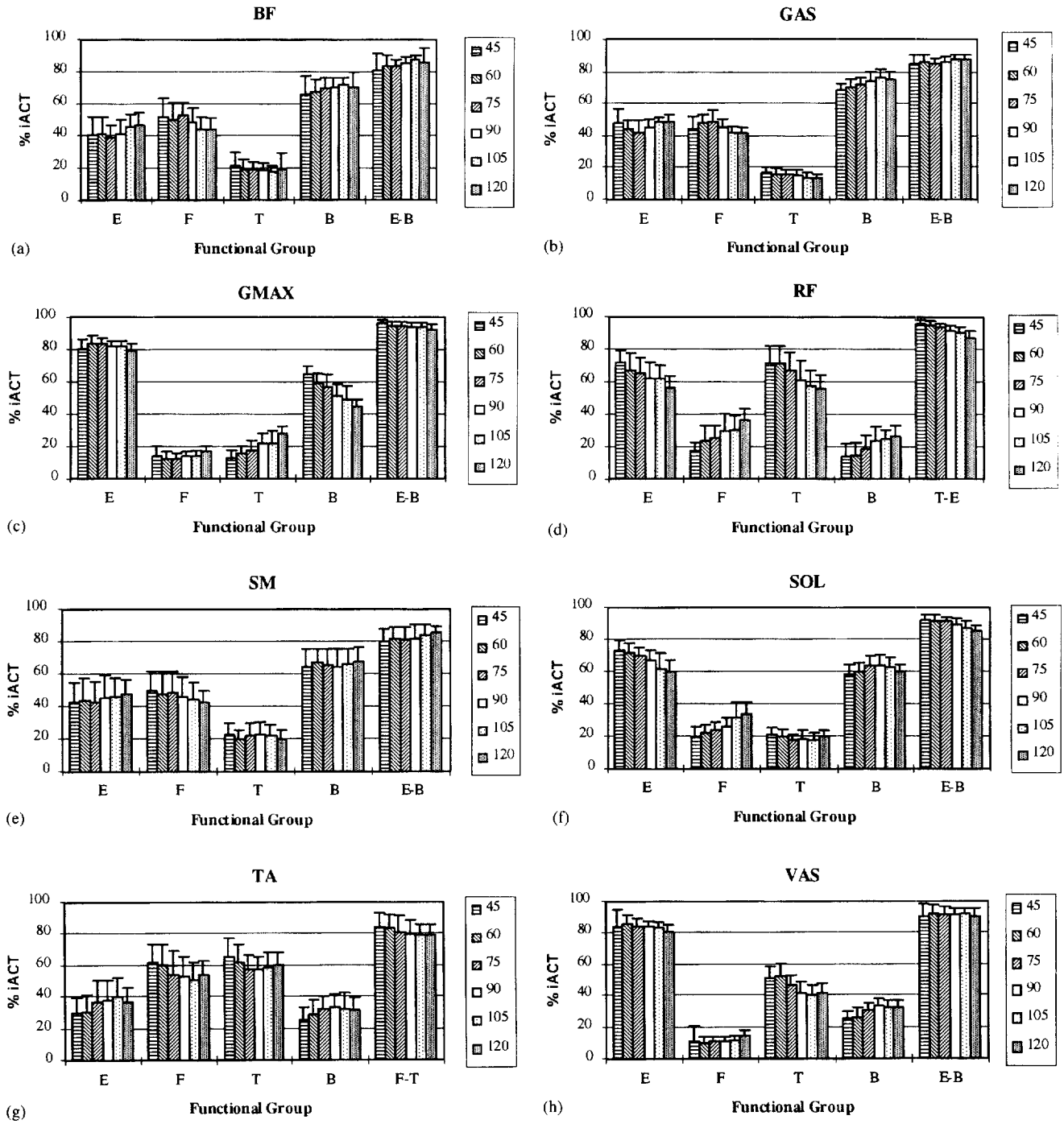

Fig. 3. The percentages of integrated muscle activation (iACT) within the four primary phase-controlled functional regions and the union region (the union between adjacent primary regions) with the highest percentage of iACT across different pedaling rates. Error bars indicate 1 standard deviation.

exclusion of most activity that is not clearly within a functional region, which reduces the importance of precisely determining the activation and deactivation time constants. Literature values have ranged from 20 to 90 ms (Winters and Stark, 1988) and the determined muscle functions were independent of changes within this range.

To interpret the results of this study within the context of pedaling coordination, it is necessary to first establish the function of the individual muscles. The primary function of the hip and knee extensors GMAX and VAS, as identified by the PCFG analysis at all cadences, was to produce power to accelerate the crank during the E region. Over 80% of their activity occurred within the E region [Figs 3(c) and (h)] which is consistent with Raasch *et al.* (1997), who showed that GMAX and VAS provided 55% of all energy delivered to the crank to overcome the resistive load. While the GMAX and VAS iEMG were found to be associated with pedaling rate

(quadratic with minimum at 90 RPM and increasing linear, respectively), these power-producing muscles were not as sensitive to pedaling rate as were the transition muscles described below.

The PCFG analysis determined that the remaining muscles all had functional contributions during either the top (T) or bottom (B) transition regions at all cadences. The primary function of TA was the T region and GAS and HAMS were the B region (Fig. 3). RF and SOL were both classified as bifunctional muscles concerned with the T–E and E–B regions, respectively (Fig. 3). Previous simulation research has shown that TA and RF muscles are particularly well-suited to propel the crank through the top tranistion region, while HAMS, GAS, and SOL are well-suited for the bottom transition region (Raasch *et al.*, 1997). Raasch *et al.* (1997) also showed that the RF and HAMS produced peak power near top-dead-center (TDC) and bottom-dead-center (BDC), respectively, providing additional support for functional roles for these muscles as transition.

Changes in EMG data as cadence increases provide further evidence for the importance of transition muscle contribution to pedaling through these regions (where limb movement switches between flexion and extension). The large increases in GAS and HAMS EMG activity [Fig. 2 and Table 3] represent a pedaling-rate sensitivity that is possibly related to coping with the increasing magnitude of velocity-dependent interaction forces arising either between individual limb segments, or at the crank (Kautz and Hull, 1993). While previous studies have demonstrated pedaling-rate sensitivity in GAS, the HAMS have not always shown a significant change, particularly BF (Ericson *et al.*, 1985; Marsh and Martin, 1995). Differences with other studies might be related to either variances in experimental protocol or EMG processing.

Unlike the bottom transition muscles, the top transition muscles (TA and RF) did not increase iEMG with pedaling rate. For the bifunctional RF, the E region activity decreased as pedaling rate increased [Fig. 3(d)]. This decrease might be related to the decreased workload as pedaling rate increased at constant workrate. Perhaps the two functions changed differently, with decreased E function obscuring any changes in T function.

Classifying SOL as a bifunctional muscle appears to resolve some conflicting ideas about its function. Marsh and Martin (1995) hypothesized that SOL was workrate sensitive, which is consistent with Raasch *et al.* (1997), who observed that SOL transferred energy generated elsewhere to the crank during the downstroke. However, Ericson *et al.* (1985) found a significant increase in SOL activity with cadence and Raasch *et al.* (1997) also emphasized the aspects of its function likely to be pedaling rate dependent (transition function and ability to prevent knee hyperextension). The results of this study showed that the SOL burst narrowed and the burst onset shifted later in the crank cycle as pedaling rate increased (Table 1). Furthermore, a second burst was evident after BDC at the higher pedaling rates [Fig. 2(f)] which was consistent across subjects and also observed in previous studies (Marsh and Martin, 1995; Ryan and Gregor, 1992). Hence, these results support both ideas—SOL appears to be bifunctional (E–B) with the E function sensitive to workload (decreasing with pedaling rate) and the B function sensitive to pedaling rate (increasing F percentage with pedaling rate).

While bifunctional muscles might have changes in emphasis, activation dynamics appear to be a primary factor influencing muscle excitation as pedaling rate increases. The hypothesis that individual muscles would have a similar phase advance of EMG onset when pedaling rate increased from 45 to 120 RPM was supported for all muscles except GAS and SOL (Table 1). Although TA onset had a similar phase advance between the extreme cadences, the onset analysis showed no systematic trend in TA onset when all pedaling rates were considered (Table 1). Therefore, TA burst onset was not considered to be affected by pedaling rate, implying that phase advance to account for activation dynamics was not a primary factor influencing excitation for any of the measured muscles crossing the ankle.

Having established that BF, GMAX, RF, SM and VAS all showed similar phase advance, in contrast to the ankle muscles, the magnitude of the phase advance must be evaluated to determine if it is consistent with activation dynamics. Typical activation time constants in the literature range from 20 to 90 ms which would require an excitation phase advance of 10 to 40 degrees, respectively, as pedaling rate increased from 45 to 120 RPM. The burst onset data reasonably fit this expected range except for RF which supports the premise that RF advances more than necessary to change functional emphasis from the extension region to the top transition region.

The PCFG analysis combined with the iEMG and burst onset/offset data has proven an effective method to analyze muscle function. But not all changes in muscle function were intuitively obvious (e.g. speculation of SOL function) and clearly indicate the need for further theoretical research involving forward dynamic simulations. Forward simulations can be used to examine mechanical energy delivery and transfer between limbs and muscles and provide additional insight into changes in muscle function with varying pedaling rates.

Acknowledgements—The authors are grateful to the Shimano Corporation of Osaka, Japan and specifically Shinpei Okajima and Wayne Stetina for their continued financial support of this research.

REFERENCES

Brown, D. A., Kautz, S. A. and Dairaghi, C. A. (1995) Effects of increased speed and workload on the control of movement in persons with hemiplegia. In *Society for Neuroscience Abstracts*, Vol. 21, part 3, p. 2083, Washington, DC.

Bogey, R. A., Barnes, L. A. and Perry, J. (1992) Computer algorithms to characterize individual subject EMG profiles during gait. *Archives of Physical Medicine and Rehabilitation* **73**, 835–841.

Citterio, G. and Agostoni, E. (1984) Selective activation of quadriceps muscle fibers according to bicycle rate. *Journal of Applied Physiology* **57**, 371–379.

Delagi, E. F., Perotto, A., Iazzetti, J. and Morrison, D. (1975) *Anatomic Guide for the Electromyographer: the Limbs.* Charles C. Thomas, Springfield, IL.

DiFabio, R. P. (1987) Reliability of computerized surface electromyography for determining the onset of muscle activity. *Physical Therapy* **67**, 43–48.

Ericson, M. O., Nisell, R., Arborelius, U. P. and Ekholm, J. (1985) Muscular activity during ergometer cycling. *Scandinavian Journal of Rehabilitation Medicine* **17**, 53–61.

Goto, S., Toyoshima, S. and Hoshikawa, T. (1976) Study of the integrated EMG of the leg muscles during pedaling at various loads,

frequency, and equivalent power. In *Biomechanics V-1A*. pp. 246–252. University Park Press, Baltimore, MD.

Kautz, S. A. and Hull, M. L. (1993) A theoretical basis for interpreting the force applied to the pedal in cycling. *Journal of Biomechanics* **26,** 155–165.

Marsh, A. P. and Martin, P. E. (1995) The relationship between cadence and lower extremity EMG in cyclists and noncyclists. *Medicine and Science in Sports and Exercise* **27,** 217–225.

Neptune, R. R. (1996) Analysis of muscle function and preferred pedaling rates in steady-state cycling. Ph.D. dissertation, Department of Mechanical Engineering, University of California, Davis.

Raasch, C. C., Zajac, F. E., Ma, B. and Levine, W. S. (1997) Muscle coordination of maximum-speed pedaling. *Journal of Biomechanics* **30,** 595–602.

Ryan, M. M. and Gregor, R. J. (1992) EMG profiles of lower extremity muscles during cycling at constant workload and cadence. *Journal of Electromyography and Kinesiology* **2,** 69–80.

SAS/STAT User's Guide, version 6, 4th edn. SAS Institute, Cary, NC, 1990.

Suzuki, S., Watanabe, S. and Homma, S. (1982) EMG activity and kinematics of human cycling movements at different constant velocities. *Brain Research* **240,** 245–258.

Takaishi, T., Yasuda, Y. and Moritani, T. (1994) Neuromuscular fatigue during prolonged pedalling exercise at different pedalling rates. *European Journal of Applied Physiology* **69,** 154–158.

Winters, J. M. and Stark, L. (1988) Estimated mechanical properties of synergistic muscles involved in movements of a variety of human joints. *Journal of Biomechanics* **21,** 1027–1041.